Dual Antibacterial Effect Of *In-situ* Electrospun Curcumin Composite Nanofibers To Sterilize Drug-resistant Bacteria

Chun-Li Liu
Qingdao University
Jun Zhang
Qingdao University
Jun Yang
Qingdao University
Xiao-Han Bai
Qingdao University
Zhi-Kai Cao
Qingdao University
Chen Yang
Qingdao University
Seeram Ramakrishna
National University of Singapore
Da-Peng Yang
Quanzhou Normal University
Yun-Ze Long (yunze.long@163.com)
Collaborative Innovation Center for Nanomaterials & Devices, College of Physics, Qingdao University, Qingdao 266071, China https://orcid.org/0000-0002-4278-4515

Nano Express

Keywords: electrospinning, in-situ deposition, drug-resistant bacteria, curcumin, naofibers

Posted Date: January 13th, 2021

DOI: https://doi.org/10.21203/rs.3.rs-143392/v1

Version of Record: A version of this preprint was published at Nanoscale Research Letters on April 7th, 2021. See the published version at https://doi.org/10.1186/s11671-021-03513-2.

Abstract

Bacterial infection especially caused by multidrug-resistant bacteria still endangers human life. Photodynamic therapy (PDT) can effectively kill bacteria, and nanofiber-based PDT can effectively reduce damages to normal tissues. However, current photosensitizers coated on the surface of fibers would release to the wound causing some side effects. And nanofibers prepared by traditional method exhibiting poor adhesion on wound, which severely reduces the PDT effect due to its short-range effect. Herein, core-shell curcumin composite nanofibers are prepared by in-situ electrospinning method via a self-made portable electrospinning device. The obtained composite nanofibers show superior adhesiveness on different biological surface than that of traditional preparation method. Upon 808nm irradiation, these composite nanofibers effectively produced singlet oxygen ($^1O_2$) without curcumin fall off. After these composite nanofibers contaminated with drug-resistant bacteria, they exhibit dual antibacterial behaviors and efficiently kill the drug-resistant bacteria. These dual antibacterial nanofiber membranes with excellent adhesiveness may benefit the applications of wound infection as antibacterial dressing.

Background

Bacterial infection without timely treatment will cause septicemia and sepsis thus seriously endanger life and health [1-3]. Although antibiotic can kill bacteria, using antibiotic in long term will lead to the development of drug-resistant bacteria, such as methicillin-resistant staphylococcus aureus (MRSA) [4-6]. In this situation, it is necessary to find other strategies to kill the bacteria. Photodynamic therapy (PDT) proved to be an effective method of sterilization [7-10]. However, most photosensitizers for PDT require ultraviolet light or short wavelength excitation [11-13]. Because the penetration depth of light in organism depends on the wavelength, ultraviolet and visible light have shallow penetration, and near-infrared (NIR) light has a deeper penetration. What worse, ultraviolet light and short wavelength light will seriously burn human tissues. In order to achieve safe and antibacterial treatments in deep tissue, developing photosensitizers excited by NIR light is a demand and trend. Upconversion nanoparticles (UCNPs) can convert NIR light into short-wavelength light [14, 15]. Due to this property, photosensitizers can be designed to combine with upconversion to achieve NIR excitation. UCNPs are used as wavelength conversion station that converts NIR light to short wavelength to excite the photosensitizer and produce singlet oxygen ($^1O_2$) [16]. However, previous studies most focus on preparation of photosensitizer coated nanoparticle structure. Photosensitizer naked on the outermost layer of nanoparticles is easy to fall off [17, 18], and it also has some side effects on biological tissues because of the directly contact, such as inhibiting tissue collagen growth [19, 20]. In fact, photosensitizers can achieve sterilization is due to its production of singlet oxygen, which means that there is no need for photosensitizer to direct contact with bacteria or biological tissues. Therefore, we can design a spacer to separate photosensitizers from biological tissues so that to avoid the possible side effects.

Electrospinning is a fast and efficient method to prepare nanofibers including organic and inorganic nanofibers [21-24]. During the preparation process of nanofiber, nanoparticles are easy to combine with fibers to form composite nanofibers. There are mainly two methods to form composite nanofibers. One is doping particles inside the nanofiber [25], and the other is loading particles onto the surface of nanofibers [26, 27]. Considering the purpose of separating photosensitizers from biological tissues, incorporating photosensitizers in the nanofiber is more preferable, because photosensitizers loaded on the fiber surface is still a risk that photosensitizers may fall off. However, if nanofiber is hydrophobic that cannot infiltrate, the singlet oxygen is hard to produce and deliver to the fiber surface achieving antibacterial property [28]. But hydrophilic nanofiber is easy to dissolve when contaminated by interstitial fluid. Therefore, it is necessary to combine NIR photosensitizers with nanofibers and ensure the photodynamic nanofiber can effectively kill bacteria, especially drug-resistant bacteria.

In this study, curcumin is used as photosensitizers considering its wide sources from organism extracts. Core-shell nanostructure of UCNPs is used as wavelength transfer station, and it shows high conversion efficiency to produce $^1O_2$. The UCNPs@Curcumin composite nanofibers are prepared by in-situ electrospinning method via a self-made electrospinning device. The obtained composite nanofibers show superior adhesiveness on different biological surface than that of traditional electrospinning preparation method. Upon 808nm irradiation, these composite nanofibers effectively produced $^1O_2$ without curcumin fall out off. After these composite nanofibers contaminated with drug-resistant bacteria of MRSA, they occur dual antibacterial behaviors that effectively kill the drug-resistant bacteria.

Methods

Materials

Thulium chloride, ytterbium chloride, neodymium chloride, and yttrium chloride were purchased from Sigma Aldrich. Methanol, ethanol, cyclohexane, curcumin, dichloromethane, acetone, polyvinylpyrrolidone (PVP), polycaprolactone (PCL), and Polyethyleneimine (PEI) were bought from Sinopharm Chemical Reagents. All materials were used without further purification.

Synthesis of Core-shell $NaYF_4$:Yb/Tm@$NaYF_4$:Nd@Curcumin

Upconversion nanoparticles (UCNPs) of $NaYF_4$:Yb/Tm@$NaYF_4$:Nd were synthesized using co-precipitate methods [29, 30]. Afterwards, 200mg of as-prepared UCNPs, 90mg of PEI and 180mg of curcumin were added and dissolved in methylene dichloride. The reactants were stirred uniformly for 20h at room temperature, and obtained products were purified by centrifugation and washed twice by ethanol.

Preparation of CurcuminComposite Nanofibers Via In-situ Electrospinning

1 g of PCL, 0.16g of PVP and 0.1g of $NaYF_4$:Yb/Tm@$NaYF_4$:Nd@Curcumin were added into 5 mL of acetone. After 12 h of stirring, a homogeneous precursor solution was obtained for electrospinning. Taking 3 mL of the precursor solution in 5 mL syringe, a self-made handheld electrospinning equipment

was used for electrospinning, which consists of 0.4mm metal needle in diameter, two alkaline batteries, and high-voltage converter that can convert 3 V of battery to 10 kV for electrospinning. Electrospinning distance between collector and an electrospinning needle was about 10cm.

Detection of $^1O_2$Formation

Singlet oxygen sensor green (SOSG) was utilized to detect the $^1O_2$ formation. An 9×9 mm square of as-prepared nanocomposite fiber membrane with different concentration of UCNPs@Curcumin was added in a quartz cuvette, then 3 mL of methanol containing 25 μM of SOSG was added. Afterwards, the cuvette was irradiated under the 808nm laser with different irradiation time. The fluorescence spectrophotometer with 504 nm of excitation wavelength was used to measure the fluorescence intensity of this solution, which reflects the singlet oxygen level.

Antibacterial Assay

Drug-resistant bacteria of MRSA was used to evaluate the antibacterial ability. Briefly, bacterial strains were cultivated in the tryptic soy broth medium. The culture media containing bacterial strains was incubated on 37°C for 15h. After culturing, the concentration of bacterial strain was 1×10^6 CFU/mL. 100 μL of bacterial solutionwas placed in a 96-well plate on a sterile ultra-clean table. A piece of circular fiber membrane with 6 mm diameter was added to the plate. After 808 nm laser irradiation, the bacterial solution in the plate was diluted 10 times with sterile water. A 10 μL of diluent was placed in a nutritional agar plate to obtain evenly coated agar plate. The treated agar plate was cultured in a constant temperature bacterial incubator at 37 °C for 18 h, and then took photographs.

Characterization

TEM and SEM image were taken JEM-2010 and SU-1510 electron microscope. Fluorescence spectrum was measured on Edinburgh FLS1000 fluorescence spectrophotometer. The absorption spectrum was recorded on Shimadzu UV2550 spectrometer. Fourier transform infrared spectroscopy was taken on Nicolet iS50 spectrometer. The zeta potential was measured with WJL-608 analyzer. The hydrophilicity with sessile drop method was tested by PT-602Atest equipment.

Results And Discussion

Characterization of Nanoparticles and Composite Nanofibers

Fig. 1a shows the TEM image of $NaYF_4$:Yb/Tm@$NaYF_4$:Nd nanoparticles (UCNPs). It demonstrates a uniform size distribution of UCNPs with an average diameter of about 45 nm. After the UCNPs were coated with curcumin, **Fig. 1**b shows a core-shell structure and the curcumin shell thickness is about 5 nm. Afterwards, these core-shell curcumin nanoparticles were embeded into PCL/PVP fibers. **Fig. 1c** shows the SEM image of these composite nanofibers prepared via a self-designed handheld electrospinning device. The diameter of nanofibers prepared by this portable equipment is about 400 nm,

the fibers are continuous without fracture, and its uniformity is similar to that of the traditional electrospinning device (**Fig. S1**). It should be noted that this portable electrospinning device can be operated by two dry batteries of 1.5V (**Fig. S2**), which gets rid of the limitation of using city power supply. Combined with its other advantages of light weight (160g in weight) and small size, it will benefit outdoor usage. **Fig. 1**d shows the TEM of these composite nanofibers,it shows good dispersity of nanopartilces in the nanofibers.

The reason for coating $NaYF_4$:Nd shell on the $NaYF_4$:Yb/Tm core is that it can enhance the photoluminescence (**Fig. 2a**). Becuase there is a good overlap between fluorescence spectrum of UCNPs and UV-vis absorption spectrum of curcumin (**Fig. 2a**), which means that stronger photoluminescence of UCNPs could transfer more energy to curcumin that can benefit the exciation of photosensitizer. Moreover, introducing this $NaYF_4$:Nd shell can regulate excitation wavelength from 980nm to 808nm (**Fig. S3**), considering 808 nm has a deeper penetration depth than 980 nm in living tissue so that it could reduce undesired burns on normal tissues. FTIR measurement was further measured. As can be seen from **Fig. 2c,** stretch vibrations of C=O at 1628 cm^{-1}, C-O at 1282 cm^{-1} and C-O-C at 1028 cm^{-1} occur in the nanocomposite particles (orange line), which origin from curcumin (green line). At the same time, there is a stretching vibration of C-N at 1125 cm^{-1}, which comes from the PEI (blue line). Their molecular structure diagrams were illustrated in the appendix (**Fig. S4**). Moreover, there is a weak C=C at approximately 1660 cm^{-1}, which corresponds to the oleic acid when synthesis of UCNPs. It can demonstrate the components of UCNPs@Curcumin composite nanofibers.

Fig. 2d exhibits fluorescence decay curves of UCNPs before and after coating curcumin. It shows a decrease of fluorescence lifetime in UCNPs that decreases from 700 μs to 390 μs after coating curcumin shell. On the basis of $\gamma = 1-\tau_2/\tau_1$, in which τ_2 and τ_1 were lifetimes referring to UCNPs before and after coating curcumin, and γ was the energy transfer efficiency. Thus, γ was calculated to be 44.3%. Such high energy transfer efficiency was obtained, which on the first aspect is due to the good overlaps between absorption spectra of curcumin and photoluminescence spectra of UCNPs (**Fig. 2b**), so that non-radiative energy transfer can occur between them. The second aspect is that UCNPs have a $NaYF_4$:Nd shell that enhances the fluorescence intensity, thus increasing their spectral overlap integral area. The third aspect is that the distance between curcumin and UCNPs is the coating thickness (<5 nm), and this small distance can facilitate to generate efficient fluorescence resonance energy transfer (FRET). As high as 44.3% was obtained by this FRET method, which can also benefit the following efficient produce of $^1O_2$.

Producing $^1O_2$ from Composite Nanofibers

In order to evaluate the ability of producing $^1O_2$ in nanocomposite fibers, the SOSG method was used. We first took nanocomposite fibers with a fixed doping concentration and observed the generation of $^1O_2$ under different irradiation time. As shown in **Fig. 3a**, for a fixed concentration such as 0.2 wt%, time is a reason that can affect the generation of $^1O_2$. The longer the time is, the more $^1O_2$ are generated. However, it also shows that although the concentration of $^1O_2$ gradually increases with increasing the irradiation

time, the rise rate gradually slows down and almost to be constant after 20 min, shown as the interval of the curve was dense. This phenomenon may be due to the fast local oxygen consuming by producing $^1O_2$ with sustained NIR light radiations, resulting in a relative low oxygen level at local area, and thus decreasing rise rate of producing $^1O_2$.

To observe the influence of doping concentration on producing $^1O_2$, **Fig. 3b** was further depicted. As shown in **Fig. 3b**, for a fixed irradiation time such as 20 min, with increasing the doping concentration, more $^1O_2$ was produced. However, the rise rate of $^1O_2$ slows down when the concentration is larger than 0.20 wt%. These experimental results suggest that there is no need to infinitely increase the irradiation time and doping concentration for producing more $^1O_2$. The optimal choice is 0.20 wt% with 20 min, and thus in the following experiments will take this concentration and irradiation time.

Wettability and Adhesivity of In-situ Electrospun Nanofiber Membrane

Considering producing $^1O_2$ is a process that requires UCNPs@Curcumin nanoparticles in fiber to interact with oxygen in body fluid, thus contact angle of this fiber membrane was further tested. **Fig. 4a** shows a drop of water dropped onto the surface of this composite nanofiber membrane and its wettability after 20s. By comparison with pure PCL nanofiber membrane(**Fig. 4b**), it shows that the composite nanofiber membrane has better wettability. Interestingly, after soaking composite nanofiber membrane in phosphate buffer solution (PBS), there is no UCNPs@Curcumin was detected in PBS by absorption spectrometer, which means that there is no curcumin fall off from the fiber. The reason for it is probably due to that curcumin was coated onto the UCNPs, and thus the size of UCNPs@Curcumin (~50nm) is big enough which is not easy to penetrate the fiber. Compared with methods of photosensitizer coated on the particles or fibers, this method of firstly increasing the size of curcumin followed by doping it into the wettable fiber can effictively avoid the fall of photosensitizer, enhance the producing of $^1O_2$ and its diffusion. Further considering the short-range effect of photodynamic treatment and that fiber membrane prepared by traditional electrospinning method has bad adhesivity on surface (**Fig. 4c** and **Fig. S5**), it would discount the photodynamic effect because the interval betweent the fiber membrane and the surface. Fortunately, these curcumin composite nanofibers could be prepared by in-situ electrospining method with good morphology (**Fig. 1c**), and it also shows good adhesivity on differnt object surface (**Fig. 4d**). It means that photodynamic fiber is more preferable to use in-situ electrospining deposition method rather than traditional electrospining method that firstly collecting fibers membrane on foil and then pressing it onto the traget.

Dual Antibacterial Effect of Curcumin Composite Nanofibers

The plate count method was used to evaluate the antibacterial properties of composite nanofibers. As shown in **Fig. 5**, whether or not 808nm light is irradiated on fibers doped with UCNPs, there is no antibacterial property (**Fig. 5b**). **Fig. 5**a’ is the control group with only light irradiation, it shows that 808 nm light itself has no bactericidal effect. Interestingly, curcumin itself shows certain antibacterial activity

(**Fig. 5c**). Furthermore, it occurs obvious bactericidal result in fibers doped with UCNPs@Curcumin under the light irradiation (**Fig. 5d'-e'**). Combined with the results of **Fig. 3**, these bactericidal results indicate that the produced $^1O_2$ from UCNPs@Curcumin under 808nm irradiation could effectively kill bacteria. On the other hand, the antibacterial activity of curcumin with and without 808nm irradiation is the same, which is due to that the absorbance of curcumin lies in the visible range (**Fig. 2b**), so that the light of 808 nm cannot work. This was also the reason why curcumin is designed to coat on the surface of UCNPs. In addition, **Fig. 5d** and **Fig. 5e** are fibers doped with UCNPs@Curcumin at 0.15 wt% and 0.2 wt%, respectively. By comparison, it is found that the 0.2wt% group shows better bactericidal properties at 20min of light irradiation, and the antibacterial effect reached to 95%. This result is also consistent with the $^1O_2$ result in **Fig. 3**.

Conclusions

In summary, core-shell curcumin composite nanofibers are prepared by in-situ electrospinning method via a self-made portable electrospinning device. The obtained composite nanofibers show superior adhesiveness on different biological surface than that of traditional preparation method. The method of firstly increasing the size of curcumin followed by doping it into the wettable fiber can effictively avoid the fall of photosensitizer, enhance the producing of $^1O_2$ and its diffusion, which may provide inspiration for designing other photodynamic nanomaterials. After these composite nanofibers contaminated with drug-resistant bacteria, they exhibit dual antibacterial behaviors and efficiently kill the drug-resistant bacteria. These dual antibacterial nanofiber membranes with excellent adhesiveness may benefit the wound infection applications as antibacterial dressing.

Abbreviations

PDT: Photodynamic therapy $^1O_2$: Singlet oxygen

MRSA: Methicillin-resistant staphylococcus aureus

NIR : Near-infrared UCNPs: Upconversion nanoparticles

PVP: Polyvinylpyrrolidone PCL: Polycaprolactone

PEI: Polyethyleneimine SOSG: Singlet oxygen sensor green

FRET: Fluorescence resonance energy transfer

PBS: Phosphate buffer solution

Declarations

Funding

This work was supported by a grant from the National Natural Science Foundation of China (11904193, 51673103 and 51973100), and the National Key Research and Development Project of China (2019YFC0121402).

Availability of Data and Materials

The datasets generated during and/or analyzed during the current study are available from the corresponding authors on reasonable request

Authors' Contributions

CL and JZ designed the experiments. CL, JY, and XB performed the experiments. ZC and CY analyzed the data. CL and JZ wrote the manuscript, SR, DPY and YZL revised the manuscript. All authors read and approved the final manuscript.

Competing Interests

The authors declare that they have no competing interests.

Authors details

[1]Collaborative Innovation Center for Nanomaterials & Devices, College of Physics, Qingdao University, Qingdao 266071, China. [2]Center for Nanofibers & Nanotechnology, Department of Mechanical Engineering, National University of Singapore, Singapore 117574, Singapore. [3]College of Chemical Engineering and Materials Science, Quanzhou Normal University, Quanzhou 362000, China

References

[1] Gupta D, Singh A, Khan A U. (2017) Nanoparticles as efflux pump and biofilm inhibitor to rejuvenate bactericidal effect of conventional antibiotics. Nanoscale Research Letters 12: 454.

[2] Gao M, Hu Q L, Feng G X, et al. (2015) A multifunctional probe with aggregation-induced emission characteristics for selective fluorescence imaging and photodynamic killing of bacteria over mammalian cells. Advanced Healthcare Materials 4: 659-663.

[3] Currie S, Shariatzadeh F J, Singh H, et al. (2020) Highly sensitive bacteria-responsive membranes consisting of core-shell polyurethane polyvinylpyrrolidone electrospun nanofibers for in situ detection of bacterial infections. Acs Applied Materials & Interfaces 12: 45859-45872.

[4] Liu S Q, Venkataraman S, Ong Z Y, et al. (2014) Overcoming multidrug resistance in microbials using nanostructures self-assembled from cationic bent-core oligomers. Small 10: 4130-4135.

[5] Liu W, Wenbin O-Y, Zhang C, et al. (2020) Synthetic polymeric antibacterial hydrogel for methicillin-resistant staphylococcus aureus-infected wound healing: nanoantimicrobial self-assembly, drug- and

cytokine-free strategy. Acs Nano 14: 12905-12917.

[6] Lin A G, Liu Y A, Zhu X F, et al. (2019) Bacteria-responsive biomimetic selenium nanosystem for multidrug-resistant bacterial infection detection and inhibition. Acs Nano 13: 13965-13984.

[7] Liu W Z, Zhang Y X, You W W, et al. (2020) Near-infrared-excited upconversion photodynamic therapy of extensively drug-resistant Acinetobacter baumannii based on lanthanide nanoparticles. Nanoscale 12: 13948-13957.

[8] Li S W, Cui S S, Yin D Y, et al. (2017) Dual antibacterial activities of a chitosan-modified upconversion photodynamic therapy system against drug-resistant bacteria in deep tissue. Nanoscale 9: 3912-3924.

[9] Zhang Y X, Huang P, Wang D, et al. (2018) Near-infrared-triggered antibacterial and antifungal photodynamic therapy based on lanthanide-doped upconversion nanoparticles. Nanoscale 10: 15485-15495.

[10] Xu F Y, Hu M, Liu C C, et al. (2017) Yolk-structured multifunctional up-conversion nanoparticles for synergistic photodynamic-sonodynamic antibacterial resistance therapy. Biomaterials Science 5: 678-685.

[11] Borodziuk A, Kowalik P, Duda M, et al. (2020) Unmodified rose bengal photosensitizer conjugated with $NaYF_4$:Yb,Er upconverting nanoparticles for efficient photodynamic therapy. Nanotechnology 31: 465101.

[12] Zhou K, Qiu X Y, Xu L T, et al. (2020) Poly(selenoviologen)-assembled upconversion nanoparticles for low-power single-NIR light-triggered synergistic photodynamic and photothermal antibacterial therapy. Acs Applied Materials & Interfaces 12: 26432-26443.

[13] Lee S Y, Lee R, Kim E, et al. (2020) Near-infrared light-triggered photodynamic therapy and apoptosis using upconversion nanoparticles with dual photosensitizers. frontiers in bioengineering and biotechnology 8: 9.

[14] Chan M H, Pan Y T, Chan Y C, et al. (2018) Nanobubble-embedded inorganic 808 nm excited upconversion nanocomposites for tumor multiple imaging and treatment. Chemical Science 9: 3141-3151.

[15] Zeng L Y, Pan Y W, Zou R F, et al. (2016) 808 nm-excited upconversion nanoprobes with low heating effect for targeted magnetic resonance imaging and high-efficacy photodynamic therapy in HER2-overexpressed breast cancer. Biomaterials 103: 116-127.

[16] Hou Z Y, Deng K R, Li C X, et al. (2016) 808 nm Light-triggered and hyaluronic acid-targeted dual-photosensitizers nanoplatform by fully utilizing $Nd^{3(+)}$-sensitized upconversion emission with enhanced anti-tumor efficacy. Biomaterials 101: 32-46.

[17] Li Z, Qiao X, He G, et al. (2020) Core-satellite metal-organic framework@upconversion nanoparticle superstructures via electrostatic self-assembly for efficient photodynamic theranostics. Nano Research 13: 3377-3386.

[18] Chan M H, Chen S P, Chen C W, et al. (2018) Single 808 nm laser treatment comprising photothermal and photodynamic therapies by using gold nanorods hybrid upconversion particles. Journal of Physical Chemistry C 122: 2402-2412.

[19] Liang S, Sun C Q, Yang P P, et al. (2020) Core-shell structured upconversion nanocrystal-dendrimer composite as a carrier for mitochondria targeting and catalase enhanced anti-cancer photodynamic therapy. Biomaterials 240: 12.

[20] Yang M, Wang H, Wang Z H, et al. (2019) A Nd^{3+} sensitized upconversion nanosystem with dual photosensitizers for improving photodynamic therapy efficacy. Biomaterials Science 7: 1686-1695.

[21] Zhang J, Li S, Ju D D, et al. (2018) Flexible inorganic core-shell nanofibers endowed with tunable multicolor upconversion fluorescence for simultaneous monitoring dual drug delivery. Chemical Engineering Journal 349: 554-561.

[22] Zhang J, Li X, Li S, et al. (2019) Ultrasensitive fluorescence lifetime tuning in patterned polymer composite nanofibers with plasmonic nanostructures for multiplexing. Macromolecular Rapid Communications 40: 5.

[23] Zhang J, Li X, Zhang J C, et al. (2020) Ultrasensitive and reusable upconversion-luminescence nanofibrous indicator paper for in-situ dual detection of single droplet. Chemical Engineering Journal 382: 8.

[24] Zhang J, Zhao Y T, Hu P Y, et al. (2020) Laparoscopic electrospinning for in situ hemostasis in minimally invasive operation. Chemical Engineering Journal 395: 7.

[25] Yang Y, Zhu W J, Dong Z L, et al. (2017) 1D coordination polymer nanofibers for low-temperature photothermal therapy. Advanced Materials 29: 12.

[26] Nie X L, Wu S L, Mensah A, et al. (2020) FRET as a novel strategy to enhance the singlet oxygen generation of porphyrinic MOF decorated self-disinfecting fabrics. Chemical Engineering Journal 395: 11.

[27] Gandra N, Abbineni G, Qu X W, et al. (2013) Bacteriophage bionanowire as a carrier for both cancer-targeting peptides and photosensitizers and its use in selective cancer cell killing by photodynamic therapy. Small 9: 215-221.

[28] Sun L W, Song L J, Zhang X, et al. (2020) Poly(gamma-glutamic acid)-based electrospun nanofibrous mats with photodynamic therapy for effectively combating wound infection. Materials Science & Engineering C-Materials for Biological Applications 113: 10.

[29] Wang F, Deng R R, Liu X G. (2014) Preparation of core-shell $NaGdF_4$ nanoparticles doped with luminescent lanthanide ions to be used as upconversion-based probes. Nature Protocols 9: 1634-1644.

[30] Wang H, Liu Y, Wang Z H, et al. (2018) 808 nm-light-excited upconversion nanoprobe based on LRET for the ratiometric detection of nitric oxide in living cancer cells. Nanoscale 10: 10641-10649.

Figures

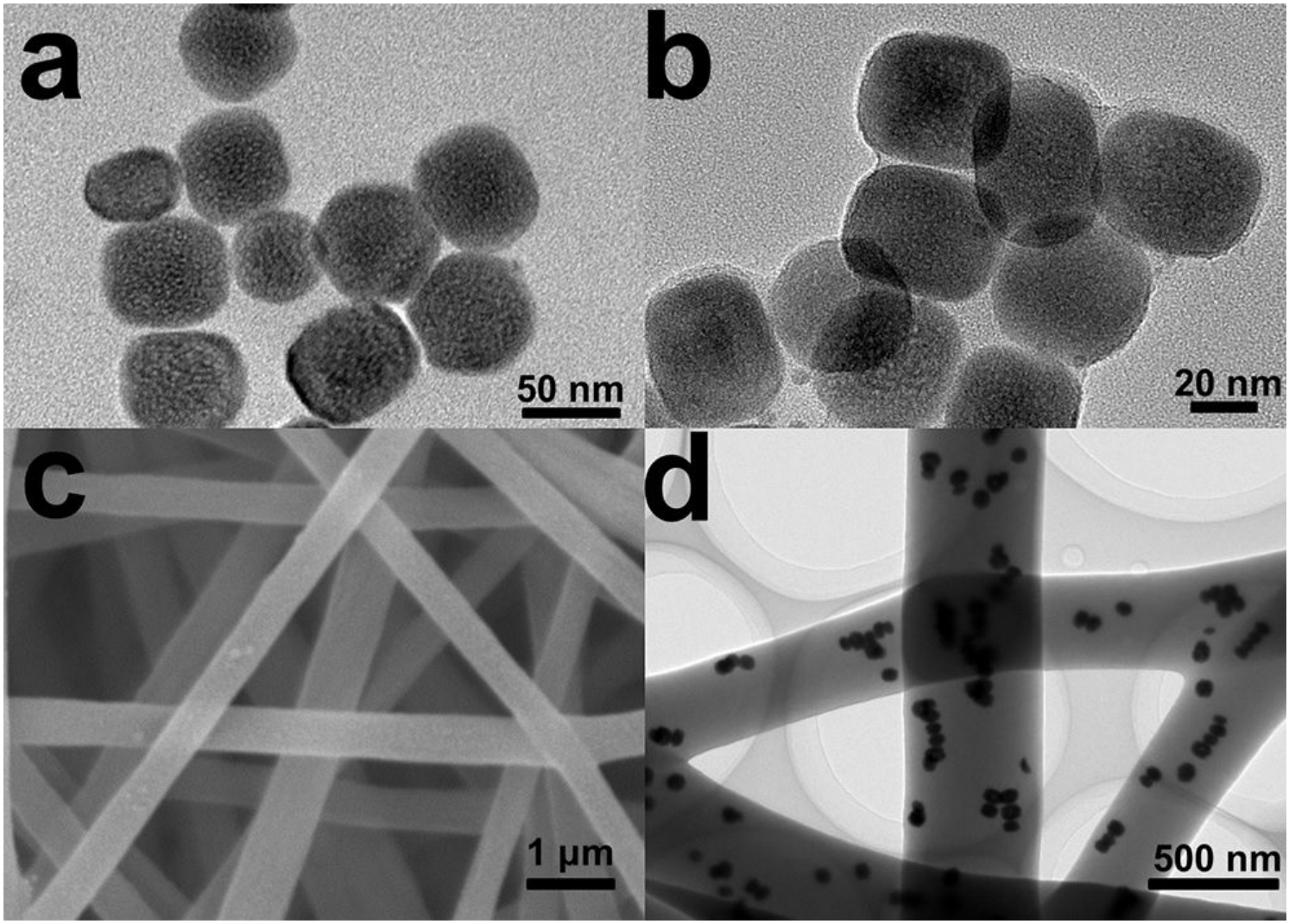

Figure 1

TEM images of (a) NaYF4:Yb/Tm@NaYF4:Nd nanoparticles (UCNPs), and (b) core-shell structured UCNPs@Curcumin nanoparticles. (c) SEM image of curcumin composite nanofibers. (d) TEM image of curcumin composite nanofibers.

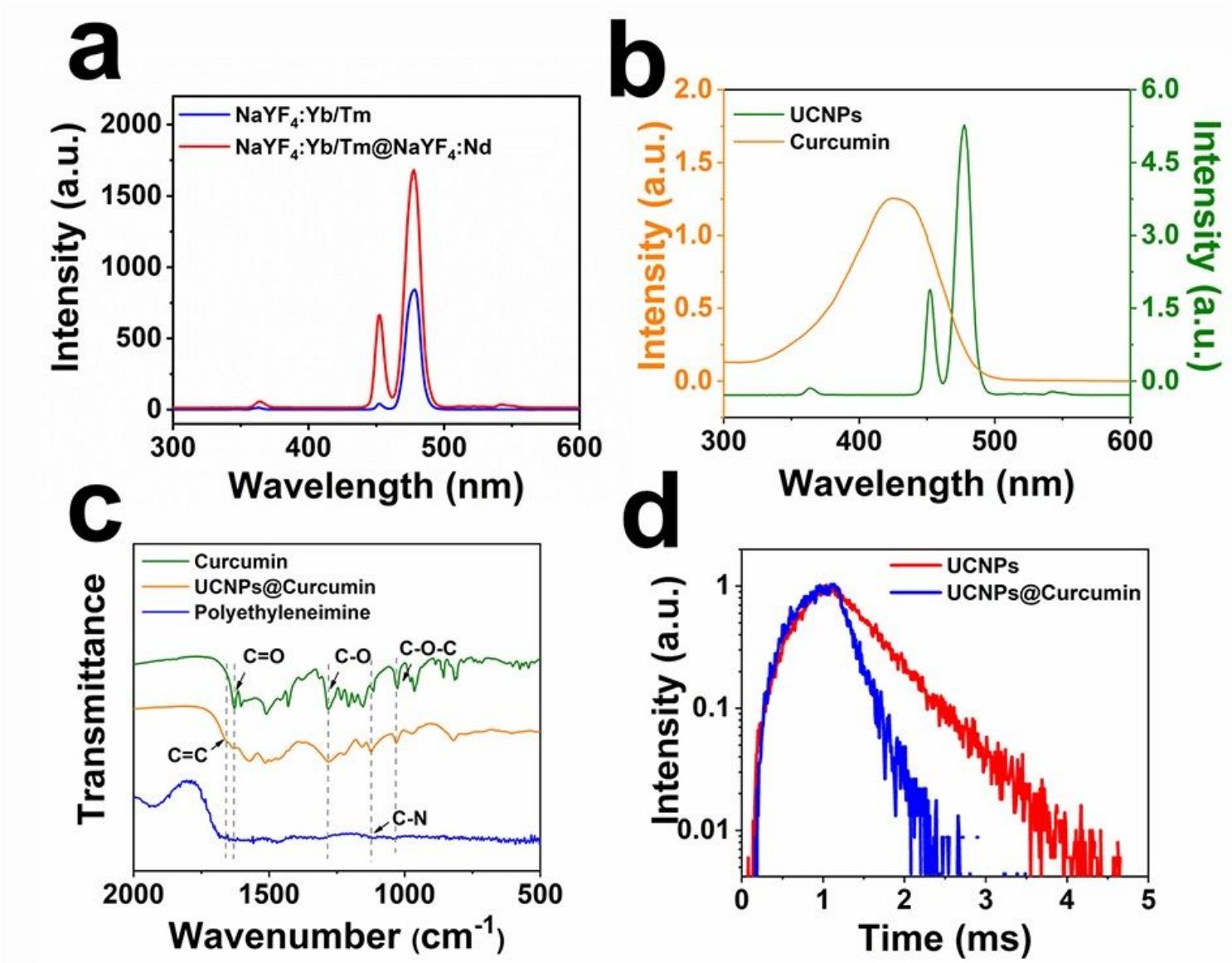

Figure 2

(a) Fluorescence spectrum of core-shell NaYF4:Yb/Tm@NaYF4:Nd excited by 808 nm. (b) Fluorescence spectrum of UCNPs and UV-vis absorption spectrum of curcumin. (c) FTIR spectra of UCNPs@Curcumin, curcumin and PEI. (d) Time-resolved fluorescence spectra of UCNPs and UCNPs@Curcumin.

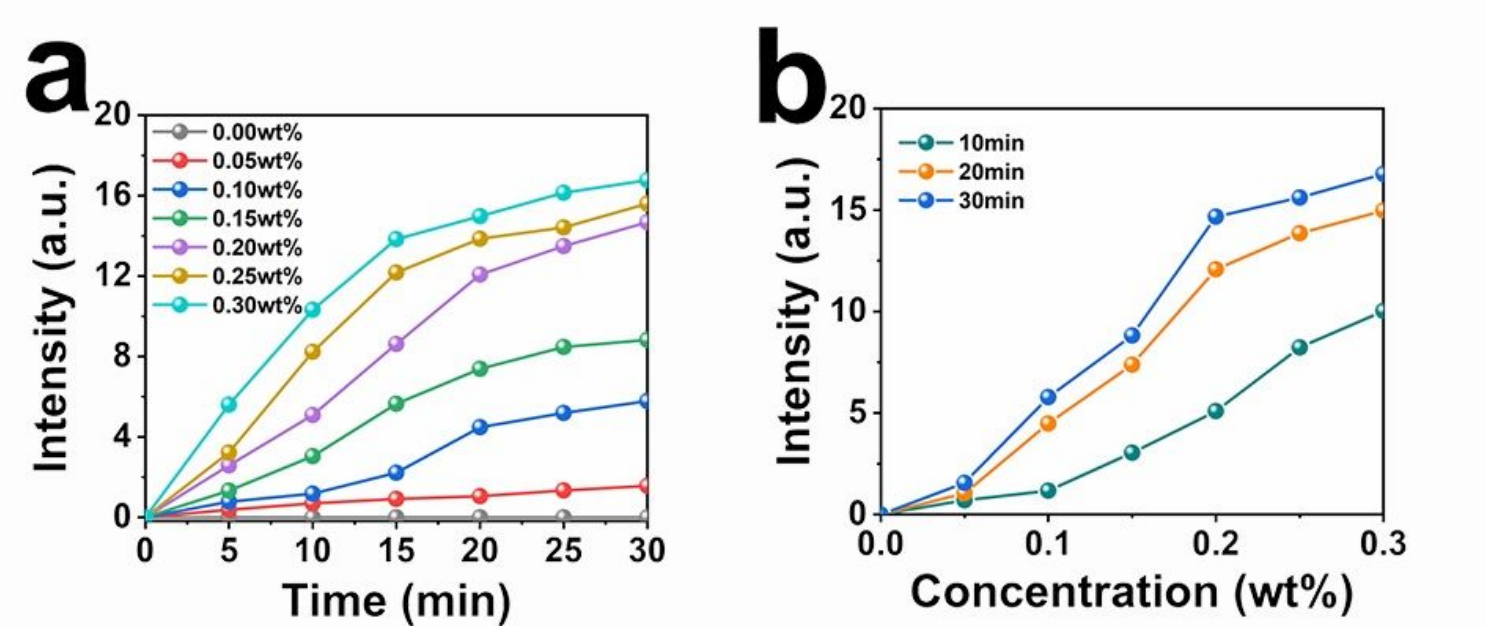

Figure 3

Singlet oxygen production of composite nanofiber membrane doped with UCNPs@Curcumin exposed to 808 nm light at different (a) concentration and (b) irradiation time.

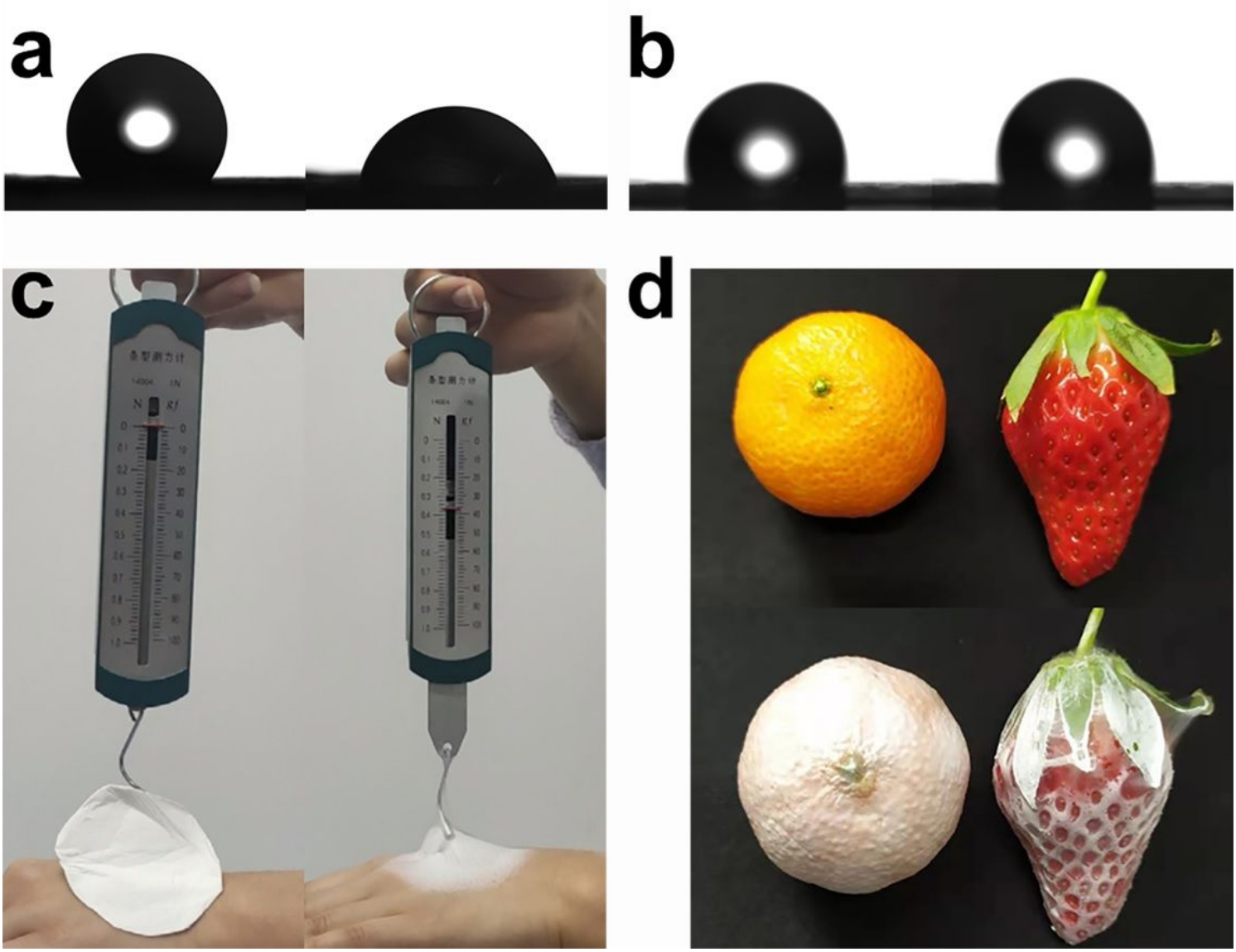

Figure 4

Water contact angle measurement of composite nanofiber membrane with matrix of (a) PCL/PVP and (b) PCL. (c) Traditional electrospun nanofiber membrane and in-situ depositon electrospun nanofiber membrane. (d) In-situ depositon electrospun on differnt object surface

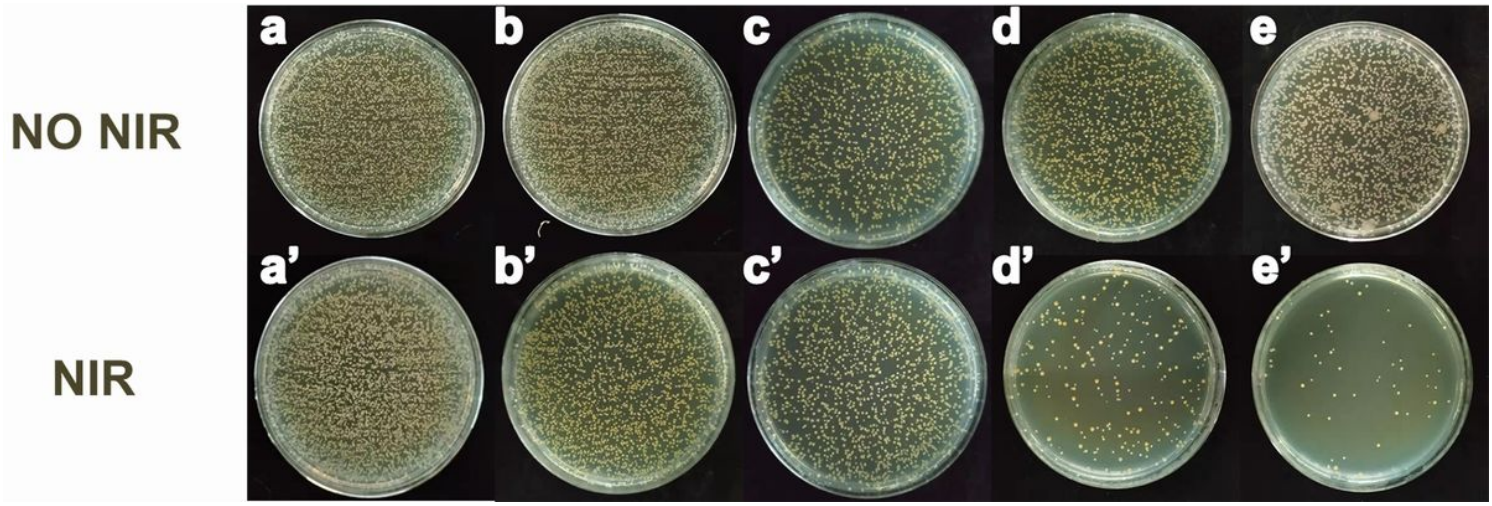

Figure 5

Antibacterial performance of nanofiber doped with different samples against MRSA (a–e) without and (a’–e’) with 808 nm light exposure: (a, a’) control group, (b, b’) UCNPs group, (c, c’) curcumin group, (d, d’) UCNPs@Curcumin with low dose group, and (e, e’) high dose group.

Supplementary Files

This is a list of supplementary files associated with this preprint. Click to download.

- SupportingInformation.docx